Acta Sci. Pol.
Architectura 24 (2025), 289–301
aspa.sggw.edu.pl ISSN 1644-0633 (suspended) eISSN 2544-1760 DOI: 10.22630/ASPA.2025.24.20

ORIGINAL PAPER

Received: 22.08.2025
Accepted: 01.10.2025

LOCAL SCOURING PROCESSES AT A PIER ON THE WHITE NILE BRIDGE

Mohammed Ahmed Abdelbaset Elamin[1], Marta Kiraga[2]✉

[1] Faculty of Civil and Environmental Engineering, Warsaw University of Life Sciences – SGGW, Warsaw, Poland
[2] Institute of Civil Engineering, Warsaw University of Life Sciences – SGGW, Warsaw, Poland

ABSTRACT

This study evaluates global scour prediction models (HEC-18, Froehlich's) for a pier on the White Nile Bridge in Sudan, hypothesising they underestimate scour in tropical rivers with cohesive sediments and dynamic monsoonal flows. Hydrological analysis, HEC-RAS modelling, and sensitivity testing revealed significant discrepancies: the HEC-18 model predicted scour depths of 0.83–1.52 m, while Froehlich's model yielded 1.35–3.18 m. Both were substantially exceeded by a region-specific nonlinear regression model for the Nile (3.24–10.67 m), confirming the hypothesis. The results demonstrate that temperate-derived models fail to capture the White Nile's cohesive clay-silt dynamics and flood-driven sediment transport. This can lead to underestimation, potentially resulting in bridge failure or collapse. The conclusion is that locally calibrated equations and adaptive mitigation strategies are essential for accurate scour risk assessment in tropical rivers.

Keywords: hydraulic structure, bridge, sediment transport, erosion, hydraulic modelling

INTRODUCTION

Rivers are dynamic systems that shape landscapes, transport water and sediment, and sustain ecosystems. They can be formed from various sources, such as rain, snowmelt, springs, or glacial melt, which accumulate and flow downhill due to gravity. Surface runoff, which is water flowing over the ground, erodes small channels (rills) that then join to form streams (Perlman, 2016). Headward erosion is the process by which streams extend upstream by eroding softer rock or soil. This process gradually changes the river's cross-section until it reaches a point of equilibrium. Tectonic uplift creates gradients that direct river courses; for example, the Nile runs in a rift-shaped path, and its White Nile tributary originates from the tectonic basin of Lake Victoria (Talbot & Williams, 2009).

The behaviour, ecological function, and value of rivers are determined by their characteristic attributes, which depend on their geological setting, the climate, and human impact. Channel morphology refers to the shape, structure, and development of the river channel. The drainage basin, or watershed, is the geographical area from which a river system collects precipitation and surface runoff (Latrubesse et al., 2017). Sediment load is a critical physical attribute that affects channel morphology, deltaic development, and ecosystem vitality.

Sediment is carried by rivers in the form of bedload (large particles scraped along the bottom), suspended load (fine clay and silt held in the water column), and dissolved load (ions from chemical weathering)

Mohammed Ahmed Abdelbaset Elamin https://orcid.org/0009-0000-3845-2203;
Marta Kiraga https://orcid.org/0000-0001-9729-4209
✉marta_kiraga@sggw.edu.pl

(Wang & Yang, 2016). The flow regime defines a river's hydrological attributes, including seasonal peaks, baseflows, and climatically dominated events (Wrzesiński & Graf, 2022). Water quality – an essential hydrological characteristic – describes the chemical, physical, and biological properties of river water (Ejigu, 2021). Rivers are also biodiversity hotspots and ecological powerhouses, supporting rich food webs and specialised environments for aquatic and terrestrial ecosystems (Junk et al., 2018).

Building on the understanding of river dynamics, it is important to examine the specific processes of erosion caused by flowing water. Water scouring is the erosional removal of sediment around hydraulic structures. Oscillatory wake vortices generate low-pressure zones that lift sediment, contributing significantly to scouring. For example, vortices have been shown to account for 30% of storm surge scour at North Sea monopiles (Sumer & Fredsøe, 2002). Scour initiation occurs when the hydrodynamic bed shear stress surpasses the critical limit for sediment entrainment (Van Rijn, 1993). The magnitude of scour is directly influenced by hydraulic factors such as debris, turbulence, unsteady flow, flood magnitude and frequency, and flow depth. Debris in flash floods can decrease scour depth by 0–54.2% by changing flow patterns (Maimun, 2024). Sediment characteristics are also important; cohesive soils (clay/silt) are more resistant to erosion than non-cohesive soils (sand/gravel) due to their cohesive forces and plasticity. A 10% increase in clay content, for instance, results in a 5.5% reduction in scour volume under continuous flow (Boivin, Garnier & Tessier, 2004). Well-graded soils also improve erosion resistance through dense particle packing. Pier geometry controls scour by altering flow patterns. Streamlined shapes (circular, triangular) minimise flow separation and vortex strength, reducing scour depths by 20–40% compared to rectangular piers (Melville & Coleman, 2000; McKeogh & Bekic, 2010a; McKeogh & Bekic, 2010b; McKeogh & Bekic, 2010c). Larger pier widths increase scour by approximately 55% for a doubled width (Lauchlan & Melville, 2001), while a skewed alignment can deepen scour by 1.5 times due to prolonged flow exposure (Richardson & Davis, 2001).

Given these complex factors, a variety of methods have been developed to predict scour. Scour prediction methods are categorised into three types, with empirical models being widely used for their simplicity. These models leverage field or lab data to correlate scour depth with variables like flow velocity, sediment size, and structure geometry. Examples include the standardised HEC-18 formula for bridge piers (Richardson & Davis, 2001), Laursen's live-bed equation, and Breusers' shape-influenced equation. While valuable where data is scarce, such as the modified HEC-18 application for the bimodal Nile sediments at Sudan's Merowe Dam spillway, they can underpredict by 20–40% in complex conditions like the cohesive clay beds at Egypt's Aswan High Dam (Elsaeed, Elsersawy & Ahmed, 2015). To overcome these limitations, hybrids combine empirical foundations with data-driven techniques: the EPRI model achieved 85% accuracy at the Blue Nile's Roseires Dam (Omer et al., 2015), and random forest-enhanced HEC-18 reduced errors below 15% at Ethiopia's Tekeze Dam using satellite data (Gebremichael et al., 2022), though conflicts in Sudan hinder long-term calibration, necessitating future focus on localised data and adaptive methods for climate-altered flow extremes exceeding historical designs.

MATERIAL AND METHODS

The study employed hydrological analysis, geotechnical profiling, and HEC-RAS hydraulic modelling to evaluate scour risk at the planned White Nile Bridge. Three empirical equations: HEC-18, Froehlich's, and a Nile-specific regression were applied, with sensitivity testing performed to assess parameter influence on predicted scour depths.

Study area

The White Nile Bridge – also known as the Omdurman Bridge – is a project that aims to improve traffic congestion between Khartoum and Omdurman by constructing a new bridge. The bridge is located 1,400 m upstream from an existing one on the west bank (approx. 15.604N, 32.482E), and 1,100 m upstream

on the east bank (approx. 15.603N, 32.496E) from another existing bridge. The route starts at Al Arbaeen Road in Omdurman, crosses over the mentioned road, and ends at its connection point with Al Gaaba Road in Khartoum (Japan International Cooperation Agency, 1990; Fig. 1).

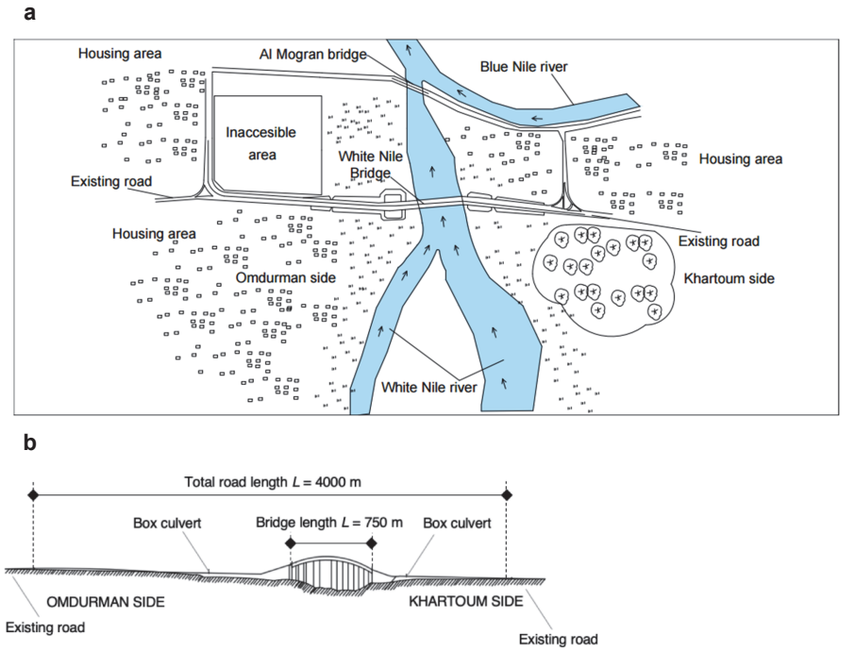

Fig. 1. The White Nile Bridge location, connecting Omdurman and Khartoum: a – plan view, b – profile view

Source: own work.

Hydrological analysis

The White Nile also possesses contrasting hydrological and sediment transport regimes, recording a mean peak discharge of approximately 2.6 million $m^3 \cdot s^{-1}$ in September and flow velocities ranging from 0.35 $m \cdot s^{-1}$ to 1.32 $m \cdot s^{-1}$. Sedimentologically, the river is characterised by pale grey clay and fine silt that account for the pale colour of the river and from which the river derives its name. However, the White Nile contributes less than 20% of the total suspended sediment load to the Nile system at the Mogran confluence because of the smaller grain size and smaller amount of its sediment compared to the coarser, mineral-rich sediments transported by the Blue Nile. This imbalance is also exacerbated by anthropogenic interventions; the construction of the Jebel Aulia Dam has significantly reduced downstream sediment transport via trapping mechanisms, altering natural sediment flux processes. As it stands, the dam's regulation has not only reduced sediment supply to downstream environments but also influenced channel form and agricultural productivity in the region (Japan International Cooperation Agency, 1990).

Subsoil condition

The subsurface profile at the project site consists of alluvial deposits overlying bedrock, with three distinct clay layers identified. The uppermost layer, ACL1 clay (the first layer of clay), is a recent riverbed deposit a few metres thick, exhibiting a very loose, soft consistency with an SPT N-value (standard penetration test) of 1,

indicative of low bearing capacity and high compressibility. Directly beneath this lies ACL2 clay (the second layer of clay), a homogeneous clay containing minor silt content. With an average SPT N-value of 5, this layer demonstrates moderate consistency and shear strength, offering limited stability for lightweight foundations when reinforced. Both layers reflect recent fluvial deposition, with ACL1's instability posing challenges for construction without ground improvement.

The third layer is ACL3 clay (the third layer of clay). This stratum is notably hardened due to desiccation and weathering, resembling a cement-like structure under normal conditions. SPT N-values range from 6 to 11, signalling higher density and load-bearing capacity compared to the upper layers. While stable in dry periods, prolonged flooding may temporarily weaken its integrity. Overall, the stratigraphy transitions from soft, unstable surface sediments to increasingly consolidated materials with depth, positioning ACL3 as the most viable layer for foundational support, provided seasonal hydrological risks are mitigated (Japan International Cooperation Agency, 1990).

HEC-RAS modelling

HEC-RAS, a free and widely used software package from the U.S. Army Corps of Engineers (USACE), employs 1D (Saint-Venant equations) and 2D (shallow water equations) hydrodynamic modelling to simulate river flow, predict flood hazards, design infrastructure, and analyse sediment transport/scour. This study utilised HEC-RAS to develop a rating curve (stage-discharge relationship) for the White Nile, integrating geometric data from satellite DEMs and Google Earth-profiled cross-sections (spaced 250–300 m) throughout the bridge downstream, including bank stations, thalweg elevation, and floodplain boundaries, along with bridge geometry (pier spacing/width) input via its bridge culvert tool (Khalafalla & Ali, 2020). A constant Manning's n = 0.03 was assigned to the channel and floodplain based on the Nile clay bed literature. Steady-flow simulations were executed across four key discharges (370 $m^3 \cdot s^{-1}$, 961.5 $m^3 \cdot s^{-1}$, 2,700 $m^3 \cdot s^{-1}$ and 12,800 $m^3 \cdot s^{-1}$) derived from historical data (Japan International Cooperation Agency, 1990), with upstream discharge boundaries and downstream water surface elevation (WS) boundaries set at 373.54 m, 375.00 m, 376.64 m, and 379.96 m, respectively, generating water surface profiles. The resulting nonlinear rating curve (discharge range of 370–12,800 $m^3 \cdot s^{-1}$) was validated by comparing simulated velocities against recorded velocities at low, normal, and high flows.

Empirical scour models

HEC-18 equation (Johnson & Torrico, 1994)

The Federal Highway Administration manual (HEC-18) is designed to provide information to estimate bridge scour. It's the most widely used equation to predict scouring in clear water channels. It uses the flow velocity, pier width, and sediment size to determine the depth of scouring on the bed of the channel (Eq. 1):

$$y_s = 2K_1K_2K_3\left(\frac{a}{y_1}\right)^{0.65} \mathrm{Fr}^{0.43}, \tag{1}$$

where:
y_s – scour depth [m],
K_1 – correction for the pier nose shape [-] (Table 1),
K_2 – correction for the angle of flow [-] (Table 2),
K_3 – correction for bed conditions [-] (Table 3),
a – pier width [m],
y_1 – flow depth [m],
Fr – Froude's number [-].

Table 1. Correction factors K_1 for different pier nose shapes for the HEC-18 equation

Shape of the pier nose	K_1 [-]
Square nose	1.1
Round nose	1.0
Circular cylinder	1.0
Group of cylinders	1.0
Sharp nose	0.9

Source: Johnson and Torrico (1994).

Table 2. Correction factors K_2 for flow attack angles and pier aspect ratios L/a for the HEC-18 equation

Angle	$L/a = 4$	$L/a = 8$	$L/a = 12$
0°	1.0	1.0	1.0
15°	1.5	2.0	2.5
30°	2.0	2.75	3.5
45°	2.3	3.3	4.3
90°	2.5	3.9	5.0

Source: Johnson and Torrico (1994).

Table 3. Correction factors K_3 for pier scour depth based on bed conditions and dune height H for the HEC-18 equation

Bed condition	Dune height [m]	K_3 [-]
Clear-water scour	not available	1.1
Plane bed and anti-dune flow	not available	1.1
Small dunes	$3.0 > H \geq 0.6$	1.1
Medium dunes	$9.2 > H \geq 3.0$	1.2–1.1
Large dunes	$H \geq 9.2$	1.3

Source: Johnson and Torrico (1994).

Froehlich's equation (Froehlich, 1988)

Froehlich's equation was developed by obtaining data from various publications, assuming the uniformity of the sediment and taking into account the median grain size of the riverbed. To correct imperfections and errors, a factor of safety has been assumed to determine the maximum scour depth (Eq. 2):

$$\frac{d_s}{a} = 0.32\,\phi \left(\frac{a'}{a}\right)^{0.62} \left(\frac{y_1}{a}\right)^{0.46} \mathrm{Fr}^{0.20} \left(\frac{a}{d_{50}}\right)^{0.08}, \tag{2}$$

where:
d_s – depth of local scour measured from a projected stream elevation [m],
ϕ – shape factor [-] (Table 4),
a' – pier width projected into the flow direction [m],
Fr – Froude's number [-],
d_{50} – median grain size of the riverbed material [m].

Table 4. Correction factors ϕ for pier shape for Froehlich's equation

Shape of the pier	ϕ [-]
Square nose	1.3
Round nose	1.0
Sharp nose	0.7

Source: Froehlich (1988).

Nile nonlinear regression analysis equation (Helal, El Sersawy & Abdelbaky, 2022)

This equation was developed by a team of engineers at Menoufia University in Egypt. It was created by analysing actual scouring data of the Nile in Egypt using SPSS software. The equation showed more accurate results for both steady and unsteady flow. The equation was given as follows (Eq. 3):

$$y_s = \frac{AQ^{0.203}V_m^{1.087}}{d_{50}^{1.805}y_{max}^{0.635}S_e^{0.073}y_1^{0.489}T^{0.156}}, \tag{3}$$

where:
A – constant parameter; $A = 4.36 \cdot 10^{-6}$ [-],
Q – water discharge [$m^3 \cdot s^{-1}$],
V_m – average velocity of flow [$m \cdot s^{-1}$],
y_{max} – maximum channel flow depth [m],
S_e – bed slope [-],
T – top width of the channel [m].

Sensitivity analysis

Sensitivity analysis was performed to quantify the effect of certain input parameters on predictions of scour depth and to test the robustness of the empirical models under Sudan's evolving hydrological and geotechnical conditions. Some of the key variables tested included flow velocity, each of which was systematically varied within realistic ranges based on historical data and regional literature (Eq. 4):

$$\Delta x = \frac{x_2 - x_1}{x_1} 100\%, \tag{4}$$

where:
Δx – percentage of change in the value [%],
x_1 – certain value,
x_2 – estimated value.

The relative influence of key input parameters on the predicted scour depth (y_s) was calculated by analysing the flow depth (y_1) and the flow velocity (v), which are hydraulically linked through the stage-discharge rating curve developed in HEC-RAS. To isolate the effect of flow depth, y_1 was incrementally increased by 10 cm (0.1 m). As the water surface elevation changes, the linked flow velocity (v) also changes proportionally based on the cross-sectional geometry; therefore, a 10 cm increase in flow depth simultaneously induces a corresponding small increase in the velocity (Eq. 5):

$$\%x = \frac{\Delta x}{\Sigma \Delta X} 100, \tag{5}$$

where:
$\%x$ – percentage of influence of an input,
Δx – change of one step of the input,
$\sum \Delta X$ – summation of the change of input in the equation.

RESULTS

HEC-18 equation results

Three main flow scenarios were used to calculate the HEC-18 scour depths (y_s): lowest, normal, and highest, representing the hydrological variability of the White Nile and utilising a rating curve created by the HEC-RAS computer to mimic the progression of flood stages through incremental adjustments in water level. Historical discharge records served as the basis for these scenarios. The analysis's main conclusion was that there was a definite inverse link between scour depth (y_s) and flow depth (y_1). Predicted scour is increased at shallower depths because flow velocity becomes more concentrated close to the riverbed. For instance, the estimated scour depth reached y_s = 1.524 m under the lowest flow circumstances (y_1 = 1.87 m), indicating severe localised turbulence. In contrast, the scour depth decreased to y_s = 0.83 m (45% decrease) under the greatest flow scenario (y_1 = 8.17 m) since the deeper flow dispersed energy throughout a larger cross-sectional area, mitigating erosive forces (Fig. 2). Despite higher velocities during peak flows (e.g., v = 1.35 m·s^{-1}), the dominant influence of y_1 suppresses scour depth (Tables 5 and 6).

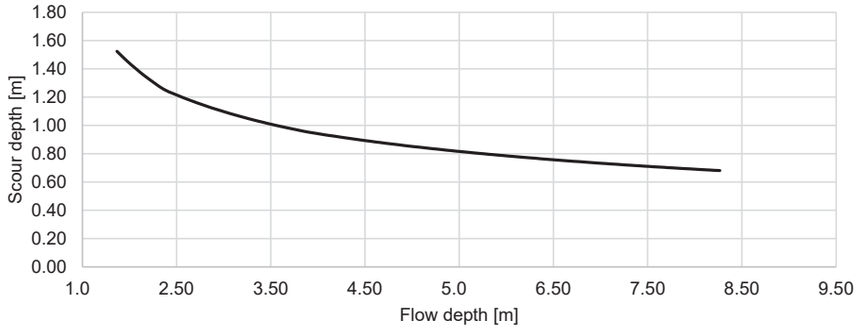

Fig. 2. The relationship between flow depth and predicted scour depth using the HEC-18 equation

Source: own work.

Table 5. Calculation of the scour using the HEC-18 equation

Water level	y_1 [m]	K_1 [-]	K_2 [-]	K_3 [-]	a [m]	v [ms^{-1}]	y_s [m]	Fr [-]	Q [m^3·s^{-1}]
Lowest flow	1.87	1.1	1.0	1.1	4.8	0.35	1.52	0.082	370.0
Normal flow	3.34	1.1	1.0	1.1	4.8	0.52	1.09	0.091	961.5
Highest flow	8.30	1.1	1.0	1.1	4.8	1.35	0.75	0.150	12,800.0

y_1 – flow depth, K_1 – correction for the pier nose shape, K_2 – correction for the angle of flow, K_3 – correction for bed conditions, a – pier width, v – flow velocity, y_s – scour depth, Fr – Froude's number, Q – water discharge.

Source: own work.

The sensitivity analysis revealed that flow depth (y_1) emerged as the most influential parameter, governing approximately 90% of the variability in predicted scour depths across all models. This dominance stems from the inverse relationship between y_1 and scour magnitude: deeper flows reduce shear stress concentration around the pier, thereby dampening erosion potential (Table 6).

Table 6. Calculation of the sensitivity analysis

$y_{1\text{-}1}$ [m]	$y_{1\text{-}2}$ [m]	Δy_1 [m]	v_1 [m·s^{-1}]	v_2 [m·s^{-1}]	Δv [m·s^{-1}]	$y_{s\text{-}1}$ [m]	$y_{s\text{-}2}$ [m]	Δy_s [m]	y_1 [%]
3.5	3.6	0.1	0.48	0.49	0.01	1.0000	0.9800	−0.0140	90.7
3.6	3.7	0.1	0.49	0.50	0.01	0.9840	0.9700	−0.0140	90.7
3.7	3.8	0.1	0.50	0.51	0.01	0.9700	0.9560	−0.0130	90.7
3.8	3.9	0.1	0.51	0.52	0.01	0.9560	0.9450	−0.0110	89.0
3.9	4.0	0.1	0.52	0.53	0.01	0.9450	0.9350	−0.0100	88.7
4.0	4.1	0.1	0.54	0.50	0.01	0.9350	0.9248	−0.0100	88.7
4.1	4.2	0.1	0.55	0.56	0.01	0.9250	0.9150	−0.0098	88.7
4.2	4.3	0.1	0.56	0.58	0.01	0.9150	0.9055	−0.0095	88.7

$y_{1\text{-}1}$ – the first flow depth, $y_{1\text{-}2}$ – the second flow depth, Δy_1 – the difference between the first and the second flow depth, v_1 – the velocity of the first flow, v_2 – the velocity of the second flow, Δv – the difference between the first and the second water velocity, $y_{s\text{-}1}$ – the predicted scour depth for the first flow, $y_{s\text{-}2}$ – the predicted scour depth for the second flow, Δy_s – the difference between the first and the second scour depth, y_1 – the flow depth.

Source: own work.

In contrast, pier geometry correction factors (K_1, K_2, K_3), held constant throughout the analysis (K_1 = 1.1, K_2 = 1, K_3 = 1.1), introduced potential underestimations in complex flow scenarios. While these constants simplified calculations, they failed to account for dynamic real-world factors such as debris accumulation or evolving bedforms.

Froehlich's equation results

Froehlich's equation predicted consistently higher scour depths (d_s) than HEC-18, emphasising its sensitivity to sediment properties (d_{50} = 0.0002 m) and flow alignment (Table 7).

Table 7. Key results of Froehlich's equation for the lowest, normal, and highest flows

Flow scenario	y_1 [m]	Fr [-]	d_s [m]
Lowest flow	1.87	0.082	1.35
Normal flow	3.34	0.091	1.80
Highest flow	8.30	0.191	3.18

y_1 – flow depth, Fr – Froude's number, d_s – depth of local scour measured from a projected stream elevation.

Source: own work.

In contrast to HEC-18, scour depth exhibited a direct correlation with flow depth (y_1), reaching its maximum value of 3.18 m at the highest flow depth: y_1 = 8.30 m. This trend underscores the model's core emphasis on sediment transport capacity (Fig. 3). Scour depth increased with higher Froude's number (Fr) values, particularly during peak flows, consistent with Froehlich's established relationship between scour and flow intensity (Fig. 4).

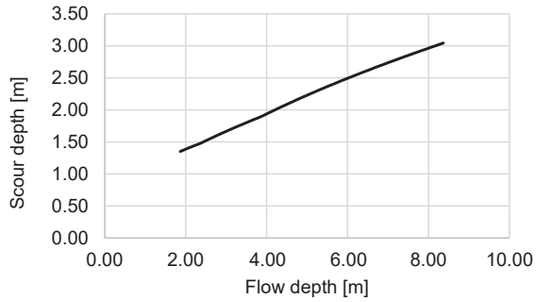

Fig. 3. The predicted scour and flow depth using Froehlich's equation

Source: own work.

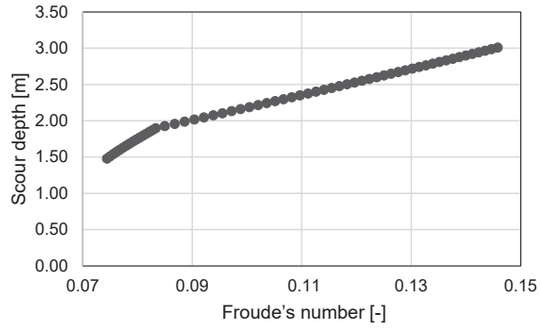

Fig. 4. Relationship between Froude's number value and predicted scour depth based on Froehlich's equation

Source: own work.

Nile nonlinear regression equation results

The Nile-specific equation, calibrated for regional sediment dynamics (d_{50} = 0.2 mm, S_e = 0.0014), yields significantly higher scour depths. This model incorporates monsoonal discharge variability (Q), maximum flow depth (y_1 = 8.296 m), and bed slope (S_e), revealing the White Nile's capacity to mobilise fine sediments during floods. The exponential rise in y_s with Q underscores the compounding effects of velocity and sediment load in Sudan's riverine environment (Table 8).

Table 8. Nile nonlinear regression equation calculation for the lowest, normal, and highest flow

A [-]	Q [$m^3 \cdot s^{-1}$]	V_m [$m^2 \cdot s^{-1}$]	d_{50} [m]	y_{max} [m]	S_e [-]	y_1 [m]	T [m]	y_s [m]
0.00000436	370.0	0.35	0.0002	8.30	0.0014	1.87	119.06	3.24
0.00000436	961.5	0.52	0.0002	8.30	0.0014	3.34	136.13	4.46
0.00000436	12,800.0	1.35	0.0002	8.30	0.0014	8.30	650.07	10.67

A – constant parameter, Q – water discharge, V_m – average velocity of flow, d_{50} – median grain size of the riverbed material, y_{max} – maximum channel flow depth, S_e – bed slope, y_1 – flow depth, T – top width of the channel, y_s – scour depth.

Source: own work.

Comparative analysis of models

The evaluation revealed significant disparities in model performance, directly tied to their underlying assumptions. HEC-18 consistently underestimated scour depths (0.83–1.52 m) compared to Froehlich's equation (1.35–3.18 m), highlighting its inherent bias toward non-cohesive sediments and a steady-state flow conditions approach misaligned with the White Nile's cohesive clay soil and dynamic monsoonal hydrology. While Froehlich's equation better captured Sudan's cohesive sediment dynamics through its explicit incorporation of grain size and flow intensity, its predictions remained conservative relative to field-validated outcomes, constrained by the absence of localised calibration for region-specific factors like seasonal sediment pulsing. Crucially, the Nile-specific nonlinear regression model (Helal et al., 2022) outperformed both, predicting scour depths of 3.24–10.67 m (Fig. 5). It demonstrates the importance of regionally calibrated equations that can adequately quantify scour risk in tropical rivers with complex sediment-transport regimes.

To assess the efficacy and applicability of various scour prediction methods under different hydraulic conditions, a scenario-based comparison was conducted. The predicted scour depths (y_s) were calculated using three distinct methodologies: HEC-18, Froehlich's equation, and a specialised Nile-specific equation. These predictions are presented for three critical flow scenarios – lowest, normal, and highest flow – derived from the Nile model, offering insights into how each method estimates scour under varying flow regimes pertinent to the Nile's hydrological characteristics (Table 9).

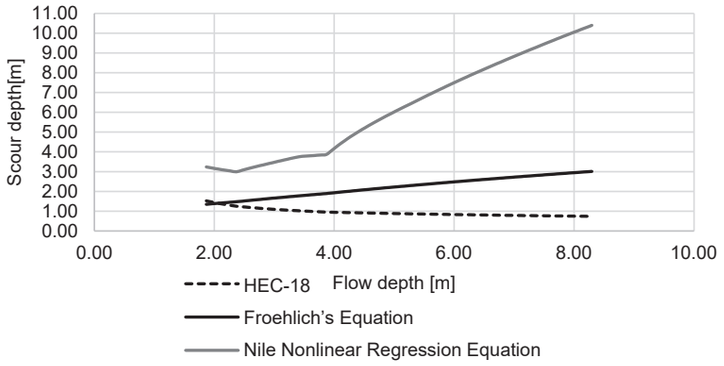

Fig. 5. Scour depth predictions versus flow depth using three methods: HEC-18, Froehlich's equation, and a Nile-specific nonlinear regression model

Source: own work.

Table 9. Predicted scour depths under different flow scenarios using HEC-18, Froehlich's equation, and the Nile-specific equation, showing scour estimates under flow from the Nile model

Flow scenario	Scour depth [m]		
	HEC-18 equation (y_s)	Froehlich's equation (d_s)	Nile-specific equation (y_s)
Lowest flow	1.52	1.35	3.24
Normal flow	1.09	1.80	4.46
Highest flow	0.83	3.18	10.67

Source: own work.

CONCLUSIONS

This study examined the applicability of global scour prediction models to Sudan's White Nile, revealing significant discrepancies in scour depth estimates. The central hypothesis guiding this research posited that globally derived empirical scour prediction models, developed primarily for temperate rivers with non-cohesive sediment and stable flows, would systematically underestimate actual scour depths in the dynamic, cohesive, and highly variable conditions of the White Nile. The HEC-18 model, widely used for bridge scour prediction, consistently underestimated scour depths (ranging from 0.83 to 1.52 m) due to its reliance on non-cohesive sediment assumptions and steady-flow conditions, which poorly align with the Nile's cohesive clay-silt mixtures and monsoonal flow variability. Froehlich's equation, while more sensitive to sediment properties, produced moderate predictions (1.35–3.18 m) but lacked calibration for the Nile's unique sediment dynamics. In contrast, the Nile-specific nonlinear regression model, incorporating localised parameters such as median sediment size (d_{50} = 0.2 mm), monsoonal discharge variability, and bed slope, predicted significantly higher scour depths (3.24–10.67 m). These findings strongly support our hypothesis, unequivocally demonstrating that temperate-derived models fall short in accurately predicting scour in tropical river systems like the White Nile. These results align with the White Nile's high sediment mobility during flash floods, underscoring the limitations of temperate-derived models.

The study faced several constraints. First, data scarcity stemming from outdated hydrological records and limited real-time sediment monitoring restricted model calibration and validation. Reliance on satellite-derived proxies introduced uncertainties, particularly in capturing subsurface sediment heterogeneity. Second, simplified assumptions in empirical models, such as constant correction factors (K_1, K_2, K_3) for pier geometry and bed conditions, overlook dynamic factors like debris accumulation and evolving bedforms, leading to potential underestimations. Third, the geographical focus on the White Nile Bridge limits the generalisability of findings to other Nile tributaries or arid wadis in Sudan, which exhibit distinct sediment and flow regimes. These limitations highlight the challenges of applying global frameworks to data-scarce, climate-vulnerable regions.

Future research should focus on expanding data collection through real-time gauging stations and sediment traps along the Nile to refine model inputs and validate satellite-derived hydrology. Hybrid approaches, integrating machine learning with empirical equations, could better capture nonlinear interactions between sediment transport and flow dynamics. Regional collaboration under initiatives like the Nile Basin Initiative is essential to harmonise transboundary sediment management and share hydrological datasets. Field testing of adaptive mitigation measures, such as gabion check dams in ephemeral wadis or sacrificial piles at high-risk bridges, would provide practical insights into cost-effective, locally tailored solutions. Expanding the scope to include other Nile tributaries and arid river systems would enhance the applicability of scour prediction frameworks across Sudan's diverse hydrological landscapes.

Development of specialised models for cohesive sediments is necessary due to the unique cohesive clay-silt mixtures of the White Nile. Integration of remote sensing and GIS for long-term monitoring is also essential. Economic feasibility studies of mitigation strategies should be included to ensure the most cost-effective and sustainable solutions are adopted. Capacity building and knowledge transfer strategies should be focused on within local engineering communities and institutions in Sudan.

Authors' contributions

Conceptualisation: M.K. and M.E.; methodology: M.E.; formal analysis: M.E.; writing – original draft preparation: M.E.; writing – review and editing: M.K. and M.E.; supervision: M.K.

All authors have read and agreed to the published version of the manuscript.

REFERENCES

Boivin, P., Garnier, P. & Tessier, D. (2004). Relationship between clay content, clay type, and shrinkage properties of soil samples. *Soil Science Society of America Journal*, *68* (4), 1145–1153.

Ejigu, M. T. (2021). Overview of water quality modeling. *Cogent Engineering*, *8* (1), 1891711.

Elsaeed, G., Elsersawy, H. & Ibrahim, M. (2015). *Scour Evaluation at the Nile River Bends on Rosetta Branch*. LAP Lambert Academic Publishing.

Froehlich, D. C. (1988). Analysis of onsite measurements of scour at piers. In *Hydraulic engineering: proceedings of the 1988 national conference on hydraulic engineering* (pp. 534–539). New York: ASCE.

Gebremicael, T. G., Deitch, M. J., Gancel, H. N., Croteau, A. C., Haile G. G., Beyene, A. N. & Kumar, L. (2022). Satellite-based rainfall estimates evaluation using a parsimonious hydrological model in the complex climate and topography of the Nile River Catchments. *Atmospheric Research*, *266*, 105939. https://doi.org/10.1016/j.atmosres.2021.105939

Helal, E., El Sersawy, H. & Abdelbaky, M. (2022). Evaluation of the predictive performance of general scour equations along the Nile River. *ISH Journal of Hydraulic Engineering*, *28* (S1), 366–379. https://doi.org/10.1080/09715010.2019.1668307

Japan International Cooperation Agency. (1990). *The feasibility study on the construction of the New White Nile Bridge in the Republic of the Sudan: Main report* (Report 52). Tokyo: Japan International Cooperation Agency.

Johnson, P. A. & Torrico, E. F. (1994). Scour around wide piers in shallow water. *Transportation Research Record*, *1471*, 66–70.

Junk, W. J., Piedade, M. T. F., Lourival, R., Wittmann, F., Kandus, P., Lacerda, L. D., Bozelli, R. L., Esteves, F. A., Nunes da Cunha, C., Maltchik, L., Schöngart, J., Schaeffer-Novelli, Y. & Agostinho, A. A. (2014). Brazilian wetlands: their definition, delineation, and classification for research, sustainable management, and protection. *Aquatic Conservation: Marine and Freshwater Ecosystems*, *24* (1), 5–22. https://doi.org/10.1002/aqc.2386

Khalafalla, E. E. & Ali, A. H. M. (2020). Inspection and rehabilitation of old White Nile steel bridge substructure. *FES Journal of Engineering Sciences*, *9* (1), 57–64. https://doi.org/10.52981/FJES.V9I1.659

Latrubesse, E. M., Arima, E. Y., Dunne, T., Park, E., Baker, V. R., d'Horta, F. M., Wight, C., Wittmann, F., Zuanon, J., Baker, P. A., Ribas, C. C., Norgaard, R. B., Filizola, N., Ansar, A., Flyvbjerg, B. & Stevaux, J. C. (2017). Damming the rivers of the Amazon basin. *Nature*, *546* (7658), 363–369. https://doi.org/10.1038/nature22333

Lauchlan, C. S. & Melville, B. W. (2001). Riprap protection at bridge piers. *Journal of Hydraulic Engineering*, *127* (5), 412–418. https://doi.org/10.1061/(ASCE)0733-9429(2001)127:5(412)

Maimun, R. (2024). Experimental study on Local Scour around Bridge Pier Models generated by Flash Floods carrying Debris. *IOP Conference Series: Earth and Environmental Science*, *1343* (1), 012028. https://doi.org/10.1088/1755-1315/1343/1/012028

McKeogh, E. & Bekic, D. (2010a). *Malahide Viaduct Reinstatement. Technical Paper 1. Collapse Mechanism and Initial Emergency Works*. Cork: Flood Study Group University College Cork.

McKeogh, E. & Bekic, D. (2010b). *Malahide Viaduct Reinstatement. Technical Paper 2. Physical Models*. Cork: Flood Study Group University College Cork.

McKeogh, E. & Bekic, D. (2010c). *Malahide Viaduct Reinstatement. Technical Paper 3. Computer Models and Hybrid Modelling*. Cork: Flood Study Group University College Cork.

Melville, B. W. & Coleman, S. E. (2000). *Bridge scour*. Colorado: Water Resources Publication.

Omer, A. Y. A., Ali, Y. S. A., Roelvink, J. A., Dastgheib, A., Paron, P. & Crosato, A. (2015). Modelling of sedimentation processes inside Roseires Reservoir (Sudan). *Earth Surface Dynamics*, *3* (2), 223–238. https://doi.org/10.5194/esurf-3-223-2015

Perlman, H. (2016). *The water cycle*. USGS Water Science School. Retrieved from https://water.usgs.gov/edu/watercycle.html [accessed: 18.05.2017].

Richardson, E. V. & Davis, S. R. (2001). *Evaluating scour at bridges* (FHWA-NHI-01-001). (4 ed.). Federal Highway Administration.

Sumer, B. M. & Fredsøe, J. (2002). *The mechanics of scour in the marine environment*. World Scientific Publishing Company. https://doi.org/10.1142/4942

Talbot, M. R. & Williams, M. A. (2009). Cenozoic evolution of the Nile Basin. In H. Dumont (Ed.), *The Nile: Origin, environments, limnology and human use* (pp. 37–60). Springer Science + Business Media. Springer Science + Business Media. https://doi.org/10.1007/978-1-4020-9726-3_3

Van Rijn, L. C., Nieuwjaar, M. W., Kaay, T. van der, Nap, E. & Kampen, A. van (1993). Transport of fine sands by currents and waves. *Journal of Waterway, Port, Coastal, And Ocean Engineering*, *119* (2), 123–143.

Wang, Q. & Yang, Z. (2016). Industrial water pollution, water environment treatment, and health risks in China. *Environmental Pollution*, *218*, 358–365. https://doi.org/10.1016/j.envpol.2016.07.011

Wrzesiński, D. & Graf, R. (2022). Temporal and spatial patterns of the river flow and water temperature relations in Poland. *Journal of Hydrology and Hydromechanics*, *70* (1), 12–29. https://doi.org/10.2478/johh-2021-0033

PROCESY LOKALNEGO ROZMYCIA PRZY FILARZE MOSTU NA BIAŁYM NILU

STRESZCZENIE

Niniejsze badanie ocenia globalne modele prognozowania rozmycia (HEC-18, Froehlicha) dla filara mostu na Białym Nilu w Sudanie, stawiając hipotezę, że dochodzi w nich do niedoszacowania rozmycia w rzekach tropikalnych z osadami kohezyjnymi i dynamicznymi przepływami monsunowymi. Analiza hydrologiczna, modelowanie HEC-RAS oraz testy wrażliwości ujawniły istotne rozbieżności: model HEC-18 przewidywał głębokości rozmycia na poziomie 0,83–1,52 m, podczas gdy model Froehlicha dawał wartości 1,35–3,18 m. Oba wyniki zostały znacząco przekroczone przez regionalny nieliniowy model regresyjny, opracowany dla Nilu (3,24–10,67 m), co potwierdziło postawioną hipotezę. Wyniki pokazują, że modele wywodzące się z klimatów umiarkowanych nie uwzględniają dynamiki kohezji iłowo-mułowej oraz transportu rumowiska. W konsekwencji dochodzi do niedoszacowania, co potencjalnie może doprowadzić do awarii lub katastrofy budowlanej mostu. Do dokładnej oceny ryzyka rozmycia w rzekach tropikalnych są niezbędne lokalnie skalibrowane równania i adaptacyjne strategie zabezpieczające.

Słowa kluczowe: budowla hydrotechniczna, most, transport rumowiska, erozja, modelowanie hydrauliczne